Modelling of Transport in Quantum Cascade Lasers and comparison with experiments

A. Leuliet, M. Carras, B. Vinter, C. Sirtori, J. Nagle

***Abstract* — A model for electronic transport in quantum cascade lasers has been developed. This allows us to determine the electronic population and the current density in a quantum cascade laser (QCL) as a function of the applied bias. The theoretical modeling has been compared with experimental Voltage-Current (V-I) curves for GaInAs/AlInAs QCL's emitting as around 9μm wavelength. A good agreement between the modeling and the experimental I-V curves and emission wavelengths is demonstrated for different doping densities.**

***Index Terms*— Quantum cascade lasers, semiconductor device models, semiconductor doping, transport.**

I. Introduction

Quantum cascade lasers (QCLs) are unipolar semiconductor devices emitting in the mid and far infrared regions (MIR and FIR respectively) of the electromagnetic spectrum. The best performance in the MIR is obtained using devices grown in the GaInAs/AlInAs//InP material system. Room temperature continuous wave operation (cw) has been demonstrated exclusively in these materials [1][2]. To improve this performance, it is also important to understand the real influence of the different parameters of the active region, such as the correct scattering times and the doping density.

II. The model

To model the transport, different formulations have been developed by different teams.[3] The scattering model provides a good compromise between accuracy and computational time. In our model, each population of the cascade structure can be obtained by solving for each state the following equations:

$$\sum_{j=1}^{N}\frac{n_j}{\tau_{ji}} - n_i\sum_{j=1}^{N}\frac{1}{\tau_{ij}} + \sum_{k=1}^{2}\sum_{j=1}^{N}\left(\frac{n_j}{\tau_{j,i+kN}} + \frac{n_j}{\tau_{j+kN,i}} - n_i\left(\frac{1}{\tau_{i+kN,j}} + \frac{1}{\tau_{i,j+kN}}\right)\right) = 0$$

where n_j are the population densities and τ_{ij} the scattering times from i to j states. Between two periods of the structure, the current density J is then given by the sum of the scatterings from the first period to the second one, minus the back filling :

$$J = e\sum_{i=1}^{N}\sum_{=1j}^{N}\left(\frac{n_{i2}}{\tau_{i2,j1}} - \frac{n_{j1}}{\tau_{j1,i2}}\right)$$

Life times result from the following intersubband scattering calculation of LO-phonon emission and absorption, roughness and alloy. The amplitudes of the last two elastic mechanisms are taken from previous work under magnetic field [7]. Scattering times are calculated by assuming a Maxwell Boltzmann distribution in the subbands due to efficient Electron/electron scattering.[8]. A corollary of these assumptions is that the current density is proportional to the doping density. We have applied an effective temperature model depending linearly with the electric power applied on the active region, according to the relationship given by [9] :

$$T_e = T_R + \alpha \times U \times I$$

where T_e is the effective electronic temperature and T_R the lattice temperature, U the voltage and J the current density.

III. The samples

To validate our approach we compared the calculated V(I) curves of four GaInAs/AlInAs samples with the same design and a targeted wavelength of 9 μm [1]. The only difference between the four samples being the doping level ranging from 10^{15} to 5.10^{15} m^{-2}. Table 1 shows some characteristics of those sample.

Doping density (m^{-2})	Threshold current ($kA.cm^{-2}$)	Emitted wavelength (μm)
1.10^{15}	1	9.4
2.10^{15}	2	9.5
4.10^{15}	5	9.7
5.10^{15}	6	10

Table I : Emitted wavelength and threshold current for the four studied samples.

The structures are processed into mesa-etched bars, 20 μm wide and 2 mm long. Current-voltage (V-I), emitted power-

current (P-I) measurements and spectra have been achieved for each sample. The current-voltage characteristics shown on figure 2 exhibits proportionality between the current and the doping density at a given voltage which confirms the validity of the Maxwell Boltzmann statistic of the electron distribution in the subbands. As expected, the threshold current increases with the doping density, which is due to additional losses introduced with the doping of the active region. In the same time, as shown on Table I, the emitted wavelength is shifted towards higher values. Let see if our transport calculation can answer this point.

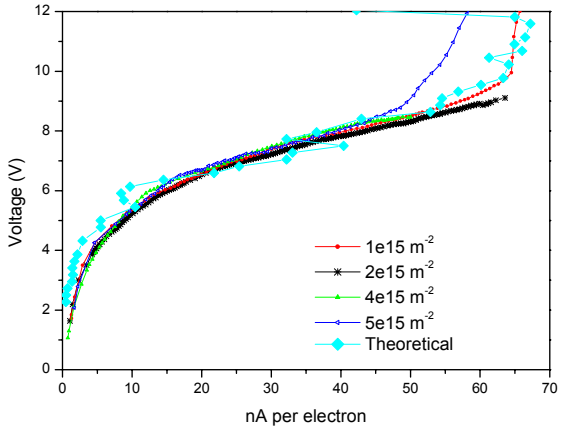

FIGURE 1: Comparison between experimental and theoretical V-I curves. The negative differential resistance appears only on the theoretical curve.

IV. Analyze on the emitted wavelength

In this part, we attempt to explain the method used to reproduce the emitted wavelength behavior as a function of the doping density. As we said before, the threshold current depends on the injector doping. For each sample, the electric field corresponding to the threshold current was investigated, and found to decrease with the doping density. By measuring the spectrum at threshold, we obtained a change in the laser alignment, resulting in a change in the emitted wavelength.

We have calculated the gain both as a function of the wavelength and the electric field, and plotted on the figure 2 the mean of this gain. The two curves show a very good quantitative agreement with a slight shift as a function of the electric field.

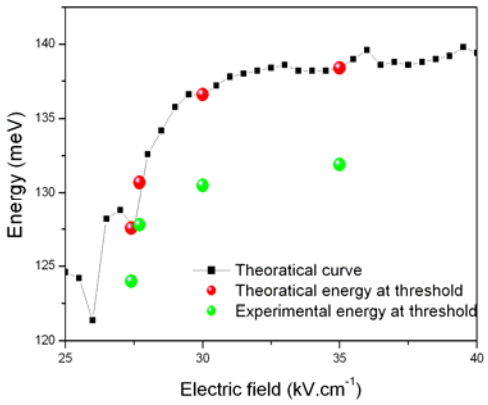

FIGURE 2 : The gain mean energy is represented by the black curve as a function of the applied electric field. The red dots show the mean energy at the electric field where the spectra have been measured. The experimental energy of the laser is represented by the green dots.

V. Conclusion

We have built a code calculating V-I curves and correlated the evolution of the emitted wavelength as a function of the doping density. This phenomenon could be used to tune the wavelength with the same design. This code is a very useful tool and could bring help for designing new structures.

References

[1] M. Beck, D. Hoffstetter, T. Aellen, J. Faist, U. Oesterle, M. Ilegems, E. Gini, H. Melchior, „Continuous wave operation of a mid-infrared semiconductor laser at room temperature“ science 295, 301 (2002).

[2] C. Faugeras, S. Forget, E. Boer-Duchemin, H. Page, J.Y. Bengloan, O. Parillaud, M. Calligaro, C. Sirtori, C. Giovannini, J. Faist, IEEE Journal of Quantum Electronics vol 41, 1430 (2005).

[3] A. Mircetic, D. Indjin, Z. Ikonic, P. H§arrison, V. Milanovic, R. W. Kelsall, “Towards automated design of QCLs” , JAP vol. 97, 084506, (2006).

[4] V.D. Jovanovic, S. Höfling, D. Indjin, N. Vukmirovic, Z. Ikonic, P. Harrison, J.P. Riethmaier, A. Forchel, “Influence of doping density on electron dynamics in GaAs/AlGaAs QCLS” JAP vol. 99, 103106, (2006).

[5] S.C. Lee, A. Wacker, “Nonequilibrium Green’s function theory for transport and gain properties of quantum cascade structures”, PRB vol 66, 245314, (2002).

[6] R. C. Iotti, F. Rossi, “Nature of charge transport in QCLs”, PRL vol. 87, 146603, (2001).

[7] A. Leuliet, A. Vasanelli, A. Wade, G. Fedorov, D. Smirnov, G. Bastard, C. Sirtori, PRB 73, 0.85311, (2006)

[8] P. Harrison, APL 75,2800, (1999)

[9] V. Spagnolo, G. Scarmacio, H. Page, C. Sirtori, “Simultaneous measurement of the electronic and lattice temperatures in GaAs/AlGaAs QCLs : influence on the optical performances”, APL vol. 84, 3690, (2004).